

A new approach to modeling the effective thermal conductivity of ceramics porous media using a generalized self-consistent method

Siroos Edrisi^{1,2} · Norollah Kasiri Bidhendi¹ · Maryam Haghghi³

Received: 17 October 2015 / Accepted: 18 April 2016 / Published online: 28 April 2016
© Springer-Verlag Berlin Heidelberg 2016

Abstract Effective thermal conductivity of the porous media was modeled based on a self-consistent method. This model estimates the heat transfer between insulator surface and air cavities accurately. In this method, the pore size and shape, the temperature gradient and other thermodynamic properties of the fluid was taken into consideration. The results are validated by experimental data for fire bricks used in cracking furnaces at the olefin plant of Maroon petrochemical complexes well as data published for polyurethane foam (synthetic polymers) IPTM and IPM. The model predictions present a good agreement against experimental data with thermal conductivity deviating <1 %.

List of symbols

A	Cross section
A_{eff}	Porous media temperature gradient
A_g	Air temperature gradient
A_m	Matrix temperature gradient
a	Air element radius
B_{eff}	Porous media constant temperature
B_m	Matrix constant temperature
b	Matrix element radius
c	Assad's model constant
C_p	Specific heat capacity at constant pressure
C_v	Specific heat capacity at constant volume
D_f	Fractal volume

D_t	Degree of capillary entanglement
g	Acceleration due to gravity
k	Heat transfer coefficient
k_{eff}	Effective heat transfer coefficient
k_g	Air heat transfer coefficient (dispersed phase)
k_m	Matrix heat transfer coefficient
Nu	Nusselt number
P	Pressure
P_{It}	A new dimensionless number defined in the present work
q	Heat flux
q_{in}	Inlet heat flux
q_{out}	Outlet heat flux
R_{nu}	A new dimensionless number defined in the present work
r	Pore radius
T	Temperature
ΔT	Temperature difference
$\frac{dT}{dy}$	Temperature gradient
T_{ref}	Reference temperature
T_w	Wall temperature
t	Time
ϑ	Body volume
v	Velocity
φ	Porosity
ρ	Density
$\rho_{T_{\text{ref}}}$	Fluid density at the reference temperature
τ	Viscous stress

✉ Norollah Kasiri Bidhendi
capepub@cape.iust.ac.ir

¹ CAPE Center, School of Chemical Engineering, Iran University of Science and Technology, Narmak, Tehran, Iran

² Maroon Petrochemical CO., Mahshar, Iran

³ Department of Chemistry, Faculty of Physics and Chemistry, Alzahra University, P.O. Box 1993891176, Tehran, Iran

1 Introduction

Thermal behavior of porous ceramic insulators made of closed cell pores has been studied in recent years. Reduction in thermal conductivity of closed cell ceramics or

insulators leads to higher energy efficiency and better reactor performance. Insulators sustain very high temperature, so they must have particular thermo-physical properties which can be used in high-temperature industrial furnaces. In the petrochemical industry in which most reactions are exothermic, usage of insulators at walls is essential in order to prevent energy loss and improving reaction yields. Thermal conductivity is the most important factor in selecting the appropriate insulator. Due to complexity in the experimental measurement of thermal conductivity, use of theoretical models is very useful and common. The thermal conductivity of the porous medium depends on the geometry as well as thermal conductivity of solid and gas phases [1]. Numerical methods, such as the finite element method, finite difference method and the Boltzmann lattice method [2] have been widely used to investigate the effective thermal conductivity of porous media. Also, several analytical models are used for prediction of thermal conductivity of porous media, and the results agree well with existing experimental data [3]. A porous media are considered as a continuous phase and the confined air in cavities plays as a disperse phase. This approach has been proposed by Hashin–Shtrikman [4]. The restrictive limits of the effective thermal conductivity of porous medium are defined [1, 2]. The upper bound refers to a continuous solid phase, including uniformly dispersed fluid filled porous media that is defined by Eq. (4). Also, the lower bound refers to a continuous fluid phase, including uniformly dispersed solid spheres as described by Eq. (5) [4]. Maxwell–Eucken considered a random distribution of pores with different diameters in porous media [4–7]. In fact the Maxwell–Eucken (Eq. 7) is arithmetically equivalent to Eq. (1). Landauer developed a model to predict effective thermal conductivity of porous media which is defined as a mixture of two phases [4–7]. The percolation model assumes a completely random distribution of solid and gas that is equivalent to an Effective Medium Theory (EMT) [8–10]. Kou et al. [3] proposed a self-similar fractal model. This is a descriptive statistical model based on numerous continuous pores in which the pore size is identified. The pores are assumed as capillary tubes that are parallel to the matrix. Capillary resistance was calculated by Capillary length and pore size and with similar electrical, porous media total resistance was obtained [11, 12]. A review of effective thermal conductivity models were given in Table 1.

The aim of this research is proposing a theoretical model to predict effective thermal conductivity of closed cell insulators, which is compatible with the experimental data. Also, experimental data are measured for insulators of Maroon petrochemical Olefin cracking unit. Meanwhile, two dimensionless numbers are also proposed which are very helpful in predicting the Nusselt number in future studies. As the proposed model demonstrates good

agreement with experimental data, it can be used for thermal modeling of high temperature reactors.

2 Theory and calculation

Among various models, the self-consistent model is the only one providing a reasonable estimation of the effective thermal conductivity and is hence a very effective model for homogeneous porous media [15]. This model predicts interaction between dispersed and continuous phases with a unit volumetric element which consist of a sphere inscribed in a bigger concentric sphere in an infinite environment. Porous medium is constituted of conjunct matrixes. For this selected element the governing equations should be solved together. Self-consistent model was given in Fig. 1 schematically.

The governing equations are represented for a representative matrix element as follows [16–18]:

Continuity equation:

$$\nabla \cdot \vec{v} = 0 \quad (11)$$

Momentum equation:

$$\nabla P = \rho_g g - \rho_g \beta (T_g - T_{avg}) \quad (12)$$

Energy equation under steady state conditions:

$$\nabla^2 T = 0 \quad (13)$$

The model is assumed steady state and heat transfer rate in the radial direction is uniform in an isotropic geometry. Due to the very low velocity of confined gas, local thermal equilibrium assumption is valid [19–22]. Energy balance is derived on a spherical matrix phase using the following simplifying assumptions:

$$\frac{\partial(\rho E)}{\partial t} + \nabla \cdot \rho v E = -\nabla \cdot q - (\nabla \cdot p v) - (\nabla \cdot [\tau \cdot v]) + \rho(v \cdot g) \quad (14)$$

at constant heat transfer rate this equation can be rewritten as Eq. 15.

$$\rho C_V \frac{DT}{Dt} = -\nabla \cdot q_i - T \left(\frac{\partial p}{\partial T} \right)_V \nabla \vartheta + \tau : \nabla \vartheta \quad (15)$$

In which subscript m represents the matrix. With the same assumptions for gas (subscript g) and extremely effective environment (subscript eff) similar relationships may be derived. Based on these assumptions the energy balance equation can be simplified in the entire element as Eqs. 16–18. The energy equations are written for confined gas and continuous ceramic phase separately.

$$\nabla^2 T_g = 0 \quad 0 \leq r \leq a \quad (16)$$

$$\nabla^2 T_m = 0 \quad a \leq r \leq b \quad (17)$$

Table 1 Review of effective thermal conductivity models

Model	Equation no.	Effective thermal conductivity	Remarks
Ohm law model [13, 14]	Equation 1	$k_{eff}(con) = k_m(1 - \varphi) + k_g\varphi$ Heat transfer direction is parallel to planes	Series–parallel configuration of porous media in 2D view
	Equation 2	$k_{eff}(con) = \frac{k_m k_g}{\varphi k_m + (1 - \varphi) k_g}$ Heat transfer direction is perpendicular to planes	
Assad's model (Geometric model) [13]	Equation 3	$\frac{k_{eff}}{k_m} = \left(\frac{k_g}{k_m}\right)^{c\varphi}$	Suitable for low porosity and c is equal to 1
Hashin–Shtrikman law model [4]	Equation 4	$k_{eff} = k_m + \frac{3\varphi k_m (k_g - k_m)}{3k_m + (1 - \varphi)(k_g - k_m)}$ The upper bound refers to a continuous solid phase including uniformly dispersed fluid filled porous media	
	Equation 5	$k_{eff} = k_g + \frac{3k_g(1 - \varphi)(k_m - k_g)}{3k_g + \varphi(k_m - k_g)}$ The lower bound refers to a continuous fluid phase including uniformly dispersed solid spheres	
Maxwell–Eucken model [7]	Equation 6	$k_{eff} = \frac{k_1 \vartheta_1 + k_2 \vartheta_2 \left(\frac{3k_1}{2k_1 + k_2}\right)}{\vartheta_1 + \vartheta_2 \left(\frac{3k_1}{2k_1 + k_2}\right)}$ k_1 : Thermal conductivity of continuous phase k_2 : Thermal conductivity of dispersed phase	Considers a random distribution of pores with different diameters
	Equation 7	$k_{eff} = \frac{k_2 \vartheta_2 + k_1 \vartheta_1 \left(\frac{3k_2}{2k_2 + k_1}\right)}{\vartheta_2 + \vartheta_1 \left(\frac{3k_2}{2k_2 + k_1}\right)}$ k_1 = Thermal conductivity of dispersed phase k_2 = Thermal conductivity of continuous phase	
Landauer's model [4]	Equation 8	$k_{eff} = \frac{1}{4} [k_g(3\vartheta_g - 1) + k_m(3\vartheta_m - 1) + ((k_g + (3\vartheta_g - 1) + k_m(3\vartheta_m - 1))^2 + 8k_m k_g)^{0.5}]$	Mixture of two phases, each phase consists of identical particles
EMT model [7]	Equation 9	$\vartheta_m \frac{k_m - k_{eff}}{k_m + 2k_{eff}} + \vartheta_g \frac{k_g - k_{eff}}{k_g + 2k_{eff}} = 0$	Equivalent to an effective medium theory (EMT)
Kou et al. [3]	Equation 10	$\frac{k_{eff}}{k_g} = \frac{(2 - D_f)\varphi \left[1 - \varphi^{\frac{D_t - D_f + 1}{2 - D_f}}\right]}{(D_t - D_f + 1)(1 - \varphi)} \left(\frac{\lambda_{max}}{L_0}\right)^{D_t - 1} + (1 - \varphi) \frac{k_m}{k_g}$	Self-similarity fractal model

$$\nabla^2 T_{eff} = 0 \quad b \leq r \leq \infty \quad (18)$$

Using the continuity of the heat flux and temperature jump conditions between the matrix and gas on the energy conservation equation, following boundary conditions are valid at the interface between the two phases.

$$T_g = T_m + \frac{k_m}{h} \left(\frac{\partial T_m}{\partial r}\right)_{r=a} \quad \text{at } r = a \quad (19)$$

$$k_m \left(\frac{\partial T_m}{\partial r}\right)_{r=a} = k_g \left(\frac{\partial T_g}{\partial r}\right)_{r=a} \quad \text{at } r = a \quad (20)$$

$$T_{eff} = T_m \quad \text{at } r = b \quad (21)$$

$$k_m \left(\frac{\partial T_m}{\partial r}\right)_{r=b} = k_{eff} \left(\frac{\partial T_{eff}}{\partial r}\right)_{r=b} \quad \text{at } r = b \quad (22)$$

The aforementioned equations are simplified only in r direction as Eqs. 23–25.

$$T_g = A_g r \cos\theta \quad 0 \leq r \leq a \quad (23)$$

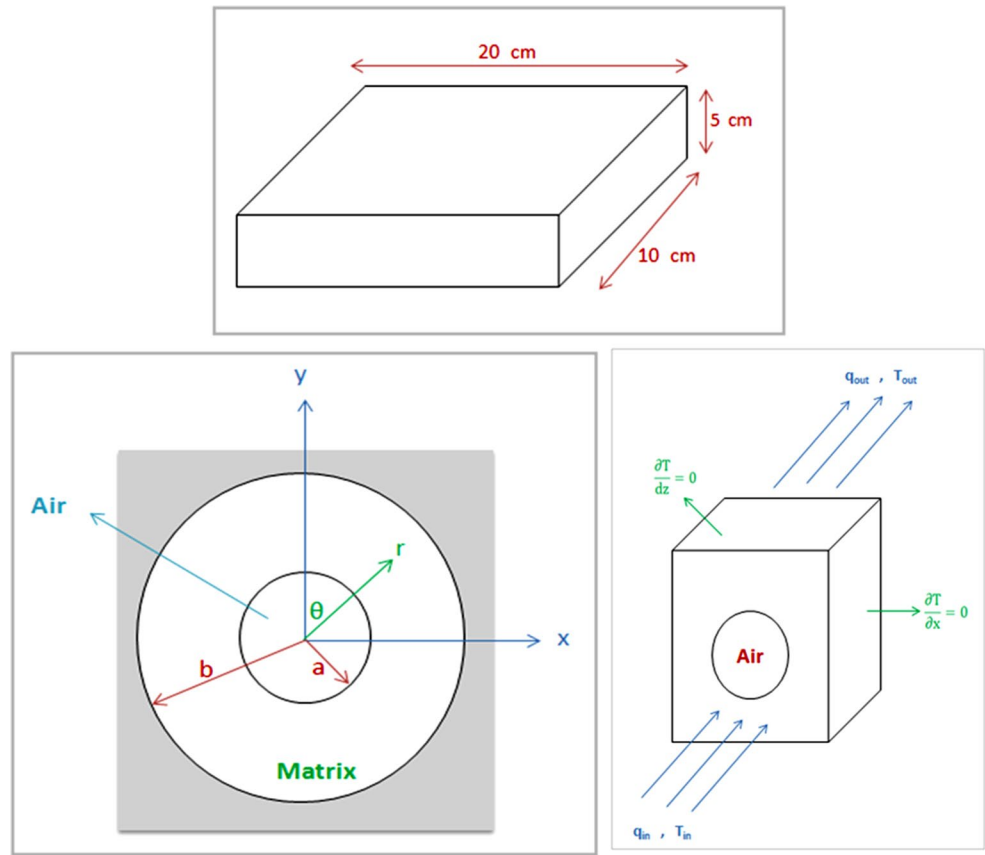
$$T_m = \left(A_m r + \frac{B_m}{r^2}\right) \cos\theta \quad a \leq r \leq b \quad (24)$$

$$T_{eff} = \left(A_{eff} r + \frac{B_{eff}}{r^2}\right) \cos\theta \quad b \leq r \leq \infty \quad (25)$$

$$A_g a^3 - A_m a^3 \left(1 - \frac{k_m}{h \cdot a}\right) - B_m \left(1 + \frac{2k_m}{h \cdot a}\right) = 0 \quad (26)$$

$$A_m b^3 + B_m - B_{eff} = A_{eff} b^3 \quad (27)$$

Fig. 1 A schematic presentation of the domain used in the self-consistent model



$$k_m A_m b^3 - 2B_m k_m + 2B_{eff} k_{eff} = k_{eff} A_{eff} b^3 \tag{28}$$

Temperatures at a and b boundaries are equal. Also, it is assumed that effective thermal conductivity of unit cell can be developed for the whole the object.

$$U = \frac{k_{eff}}{V} \left[A_{eff} \cdot b - \frac{2A_{eff} B_{eff}}{b^3} + \frac{A_{eff} B_{eff}}{b^2} - \frac{2B_{eff}}{b^5} \right] \tag{32}$$

By solving energy equation with considering the porosity of the object as being $\varphi = (\frac{a}{b})^3$, effective thermal conductivity of insulators can be represented by Eq. 33.

$$U = \frac{1}{V} \left\{ \int_{V_m - V_c} k \nabla T \cdot \nabla T dV + \int_{V_g - V_c}^{V_g + V_c} k \nabla T \cdot \nabla T dV + \int_{V_g - V_c} k \nabla T \cdot \nabla T dV \right\} \tag{29}$$

$$\nabla(T(k \nabla T)) = T k \nabla^2 T + k \nabla T \cdot \nabla T \Rightarrow \nabla(T(k \nabla T)) = k \nabla T \cdot \nabla T \tag{30}$$

$$U = \frac{1}{V} \left(\int_{S_{mo}} T_m k_m \nabla T_m \cdot \vec{n} \cdot dS + \int_{S_{mi}} T_m k_m \nabla T_m \cdot -\vec{n} \cdot dS + \int_{S_{go}} T_g k_g \nabla T_g \cdot \vec{n} \cdot dS + \int_{S_{gi}} T_g k_g \nabla T_g \cdot -\vec{n} \cdot dS + \int_{S_{gi}} T_g k_g \nabla T_g \cdot \vec{n} \cdot dS \right) \tag{31}$$

Table 2 Thermal conductivity of matrix k_m (W/mK) [24], effective thermal conductivity of insulator resulted from experimental studies k_{eff}^{exp} (W/mK) [24] and calculated effective thermal conductivity of insulator through the developed model Eq. 33

Porosity (%)	Equation 33 k_{eff}^{cal} (W/mK)	IPMT [24] k_{eff}^{exp} (W/mK)	[24] k_m (W/mK)	Porosity (%)	Equation 33 k_{eff}^{cal} (W/mK)	IPM [24] k_{eff}^{exp} (W/mK)	[24] k_m (W/mK)
30	0.39	0.45	0.62	30	0.43	0.49	0.68
35	0.36	0.4	0.62	35	0.395	0.435	0.68
40	0.33	0.35	0.62	40	0.36	0.38	0.68
45	0.3	0.31	0.62	45	0.325	0.31	0.68
50	0.27	0.27	0.62	50	0.29	0.24	0.68
55	0.24	0.24	0.62	55	0.26	0.205	0.68
60	0.21	0.21	0.62	60	0.23	0.17	0.68
65	0.18	0.2	0.62	65	0.2	0.14	0.68
70	0.15	0.18	0.62	70	0.18	0.11	0.68
SD 1.6 %				SD 2.5 %			

All values are reported at temperature 100 °C

$$k_{eff} = k_m \left[1 + \frac{3\varphi + \left(\frac{k_m}{k_g - k_m}\right) \left(\frac{k_g}{h \cdot a}\right) 3\varphi}{1 - \varphi + \left(\frac{3k_m}{k_g - k_m}\right) - \left(\frac{k_m}{k_g - k_m}\right) \left(\frac{k_g}{h \cdot a}\right) (2 + \varphi)} \right] \quad (33)$$

Two dimensionless numbers, P_{lt} (ratio of heat transfer coefficient in local thermal equilibrium to the difference between heat transfer coefficients in local thermal Non-equilibrium) and R_{nu} (Reverse Nusselt Number) are defined as follows.

$$P_{lt} = \frac{k_m}{k_g - k_m} = \frac{\text{heat transfer coefficient in LTE}}{\text{difference between heat transfer coefficients in LTNE}} \quad (34)$$

$$R_{nu} = \frac{k_g}{h \cdot a} = \frac{1}{Nu} \quad (35)$$

Then, final equation for k_{eff} is obtained as Eq. 36.

$$k_{eff} = k_m \left[1 + \frac{3\varphi(1 + P_{lt} * R_{nu})}{1 - \varphi + 3P_{lt} - (P_{lt} * R_{nu})(2 + \varphi)} \right] \quad (36)$$

3 Results and discussion

The results of the proposed model are validated in comparisons against theoretical and experimental data. Initially the present model results are compared against published experimental data [23–25]. Effective thermal conductivity of porous media like mineral polymer IPM and IPMT alumino silicates are reported on the furnace condition with different porosities [24]. It was found that the chemical composition of porous media affects the microstructure characteristics such as size and spatial arrangement of pores, homogeneity and thermal

behavior of porous matrix. In particular, homogeneity of inorganic polymer improves thermal insulation specifications. The relation between effective thermal conductivity and porosity is consistent with analytical models that were described by Maxwell–Eucken and Landauer [24]. To prepare porous geopolymers, two different compositions of metakaolin were tested with a specific Si/Al molar ratio. This was achieved by mixing different proportions of the standard and sand-rich alumino silicates. Alkaline solution was added to each powder with a solid/liquid ratio of 1.66. Finally IPM and IPMT were obtained with Si/Al molar ratios of 1.23 and 1.79 respectively. Na/Al ratio was close to 1 to achieve homogeneous slurry and balance the negative charge of alumina oligomers. The porosity and size distribution was evaluated carefully [23, 24]. Thermal conductivity is measured at different conditions using the Heat Flow Meter (ASTM C518, ISO8301). Homogeneous samples with parallel flat faces are selected. The apparatus works based on Fourier's law under steady state conditions. A thermal gradient is imposed across the sample width which is maintained between two copper plates, the upper plate is a heat source [24].

The ASTM standard C177, “Standard Test Method for Steady-State Heat Flux Measurements and Thermal Transmission Properties by Means of the Guarded-Hot-Plate Apparatus,” is used as a template and modified to accommodate the additional requirements for operation in a cryogenic environment. A single-sided guarded-hot-plate with only one cold plate and one specimen is used. The effective thermal conductivity of the samples was measured by recording the temperature on either side of the sample for a specific heater power after steady state was achieved [25–27]. Standard deviation (SD) which was calculated by following formula shows good agreement with experimental results.

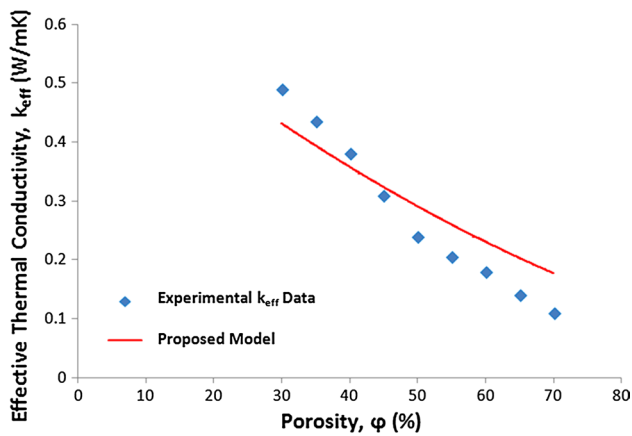


Fig. 2 Variation of effective thermal conductivities for IPM porous media against porosity (experimental and predicted)

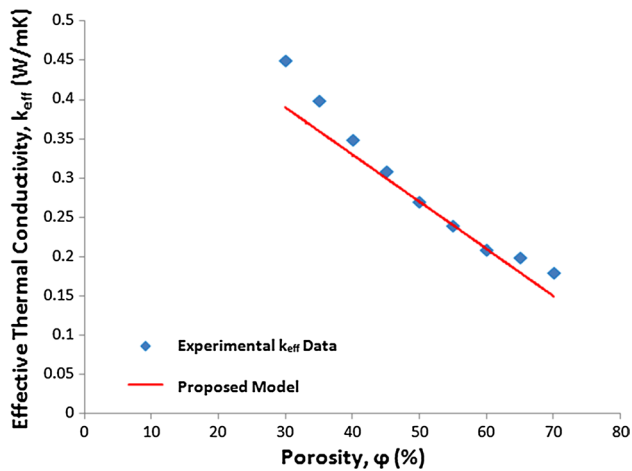


Fig. 3 Variation of effective thermal conductivities for IPMT porous media against porosity (experimental and predicted)

$$\text{Standard deviation} = \sqrt{\sum_{i=1}^n \frac{[k_{\text{eff},i}^{\text{exp}} - k_{\text{eff},i}^{\text{cal}}]^2}{n-1}} \quad (37)$$

The results show good agreement and high accuracy between experimental effective thermal conductivity and results of the model as shown in Table 2. Porosity plays a key role in effective thermal conductivity of porous media. Figures 2 and 3 show $k_{\text{eff}}^{\text{exp}}$ and $k_{\text{eff}}^{\text{cal}}$ versus porosity for synthetic polymers IPM and IPMT.

In Table 3 experimental and computed k_{eff} by Eq. 33 are compared together. Polyurethane foam with 97 % porosity, 25 mm thickness and temperature gradient of 10 K are considered.

Figure 4 and Table 3 show the comparison of model predictions of polyurethane foam versus temperature and

Table 3 Thermal conductivity of matrix k_m (W/mK) [25], effective thermal conductivity of insulator resulted from experimental studies $k_{\text{eff}}^{\text{exp}}$ (W/mK) [25], calculated effective thermal conductivity of insulator through the developed model Eq. 33 for polyurethane foam

Temperature (°C)	$k_{\text{eff}}^{\text{cal}}$ (W/mK) Equation 33	$k_{\text{eff}}^{\text{exp}}$ (W/mK) [25]	k_m (W/mK) [25]
80	0.007	0.0085	0.0011
100	0.01	0.011	0.00135
120	0.014	0.014	0.0016
140	0.012	0.015	0.00185
160	0.016	0.0165	0.0021
180	0.0175	0.018	0.0024
200	0.019	0.02	0.0027
220	0.02	0.0205	0.003
240	0.022	0.021	0.0032
260	0.024	0.0215	0.00345
280	0.026	0.022	0.0037

SD 0.08 %

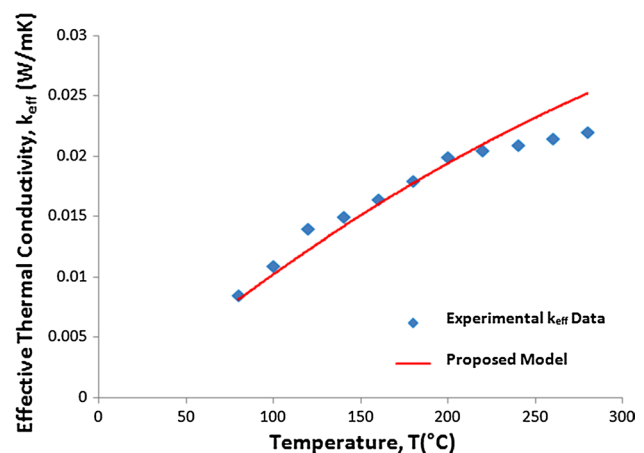


Fig. 4 Predicted and experimental results [25] for effective thermal conductivity of polyurethane foam versus temperature

experimental data. The results are very compatible and SD is very low.

Further on, different insulators are assessed and experimental data are measured. The refractory pieces of Amol Carborundum Co. products are employed in Maroon petrochemical olefin cracking unit furnaces called K26_AC4-A which is shown in Fig. 5.

Refractory insulator bricks contain different molar ratios of metal oxides such as Al_2O_3 , SiO_2 and Fe_2O_3 . The products are named as K28-AC5, K26-AC4_B, K26-AC4_A, K25-AC3 and K23-AC2. The overall density of bricks varies between 0.6 to 0.95 g/cm^3 and maximum operating temperature between 1260 °C for K23 and 1540 °C for K28. Thermodynamic properties of air and the insulator



Fig. 5 Refractory ceramic blocks used in the Maroon Petrochemical Economic Zone Mahshahr-Iran (plates 1–8 olefin unit)

Table 4 Properties of refractory ceramic blocks used in the Maroon Petrochemical Economic Zone Mahshahr-Iran (olefin unit furnace 1–8)

Grade	Unit	K23	K25	K26	K26	K28
Code factory	–	AC2	AC3	AC4-A	AC4-B	AC5
Maximum service temperature	°C	1260	1320	1380	1430	1540
Overall density	g/cm ³	0.6	0.7	0.8	0.85	0.95
Apparent porosity	%	70	65	60	60	55
Cold crushing strength	kg/cm ²	10–17	20–25	20–30	20–30	25–35
Change in length						
Time: 24 h	%	–0.7	–0.5	–0.4	–0.3	–0.3
Temp: 1450 °C		1230 °C	1300 °C	1350 °C	1400 °C	–
Chemical analysis						
Al ₂ O ₃	%	>30	>38	>45	>52	>63
SiO ₂		<62	<55	<52	<45	<35
Fe ₂ O ₃		<1	<1	<1	<1	<0.5
Alkalies		<4	<3	<2.5	<2	<1

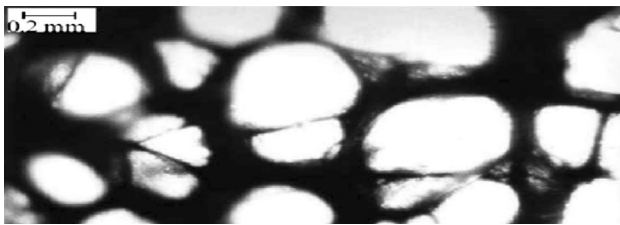


Fig. 6 SEM image of refractory ceramic blocks used in the Maroon Petrochemical Economic Zone Mahshahr-Iran (olefin unit furnace 1–8)

material have been extracted from the literatures and have been reported in Table 4 [26–31].

Figure 6 shows SEM image of an insulator brick (taken by Cambridge Stereo Scan-S360 equipped with spot analysis, EDX).

The SDs of different models relative to the experimental results are reported in Table 5. The SD of the proposed model from experimental results is about 0.5 %, which is lower than previous models demonstrating that the

proposed model can be predicted effective thermal conductivity of closed cell porous media more accurately compared to previously reported theoretical models.

In Figs. 7, 8, 9, 10 and 11, experimental results were compared to the proposed model as well as the previous models for different insulators in the temperature range 600–1300 °C. The results of k_{eff} of K26_AC4-A were plotted against operating temperature in Fig. 7. These data were reported in Table 5 too. Although the SD of the proposed model is lower than the other models, but at a temperature lower than 950 °C, Assad's model shows better agreement. Also, for temperature higher than 950 °C, the proposed model shows the best agreement with experimental data.

The k_{eff} values of K28_AC5 insulator were calculated and plotted against temperature in Fig. 8. All models showed the same behavior against temperature change. K_{eff} decreased against temperature with a mild slope from 600 to 900 °C and then increased with temperature enhancement. Landauer's model showed the most deviation from experimental data. The obtained model was predicted

Table 5 Comparing the experimental results and theoretical effective thermal conductivities estimated by different models for refractory K26_AC4-A product Amol Carborundom, used in Maroon petrochemical olefin cracking unit

Temperature (K)	(K _{eff}) Experimental (W/mK)	(K _{eff}) Proposed model (W/mK)	(K _{eff}) Ohm law model (W/mK)	(K _{eff}) Geometric and Assad's model (W/mK)	(K _{eff}) Hashin–Shtrikman law model (W/mK)	(K _{eff}) Maxwell–Eucken model (W/mK)	(K _{eff}) Landauer's model (W/mK)
600	0.154	0.657	0.825	0.455	0.704	0.975	2.026
700	0.189	0.620	0.778	0.491	0.669	0.918	1.905
800	0.224	0.616	0.771	0.546	0.666	0.910	1.886
873	0.250	0.636	0.796	0.602	0.686	0.939	1.947
900	0.259	0.644	0.806	0.625	0.694	0.950	1.969
1000	0.294	0.703	0.880	0.732	0.753	1.039	2.154
1073	0.320	0.769	0.965	0.837	0.818	1.139	2.363
1100	0.329	0.792	0.995	0.878	0.842	1.175	2.439
1200	0.364	0.913	1.150	1.078	0.962	1.359	2.823
1273	0.390	1.019	1.287	1.285	1.069	1.522	3.164
1300	0.399	1.063	1.344	1.375	1.113	1.590	3.307
SD		0.5 %	0.88 %	0.65 %	0.60 %	1.26 %	5.73 %

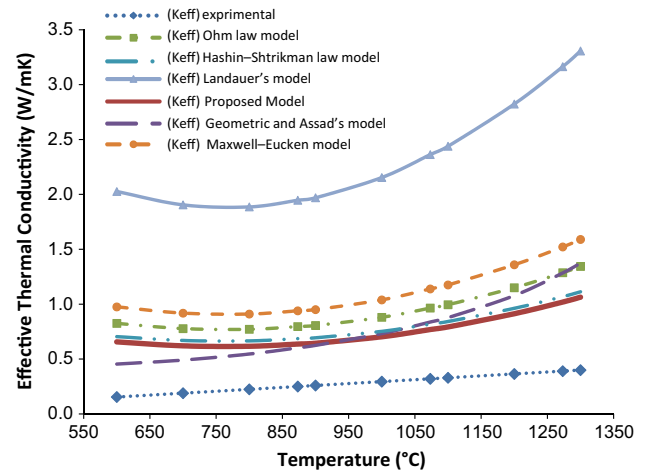


Fig. 7 Comparison of predicted effective thermal conductivity for insulator K26_AC4-A by different models and the experimental measurements

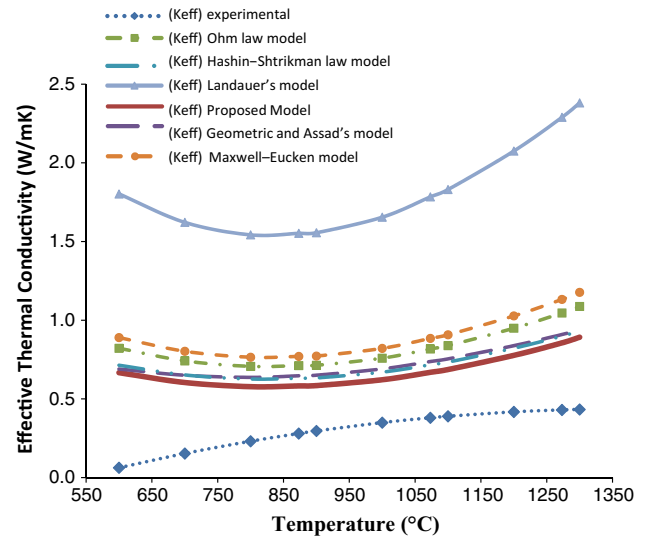


Fig. 8 Comparison of predicted effective thermal conductivity for insulator K28_AC5 by different models and the experimental measurements

effective thermal conductivity better than the other developed models.

The accuracy of different models were compared together in Fig. 9 for K26_AC4-B sample. Thermal behavior of this sample is very similar to K26_AC4-A type. This is due to the similar structure of the ceramics.

The K26_AC3 and K26_AC2 were studied in this research too. The experimental data were measured at different temperatures and were compared with different

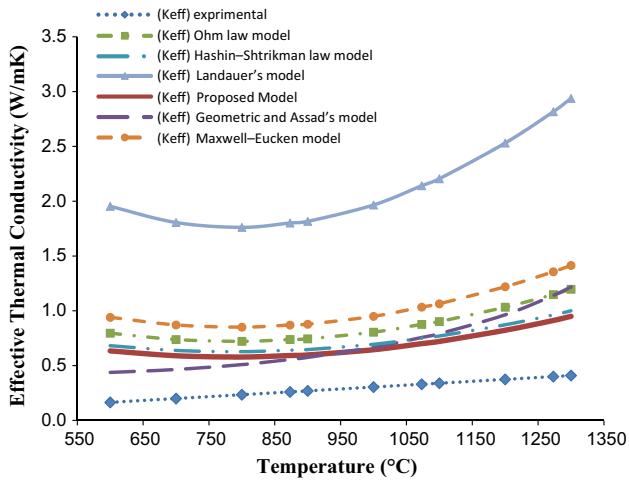


Fig. 9 Comparison of predicted effective thermal conductivity for insulator K26_AC4-B by different models and the experimental measurements

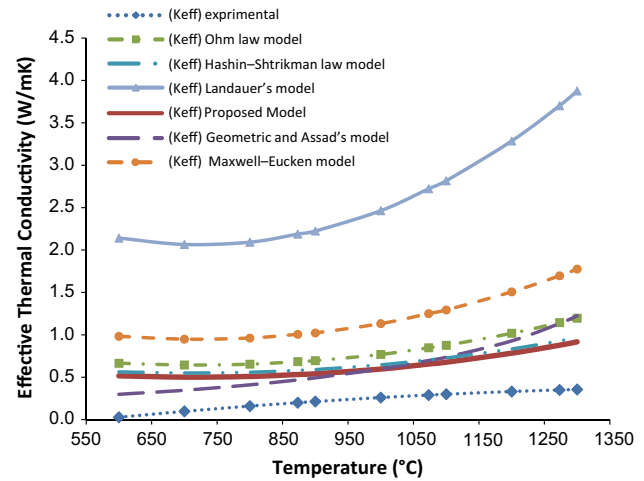


Fig. 11 Comparison of predicted effective thermal conductivity for insulator K26_AC2 by different models and the experimental measurements

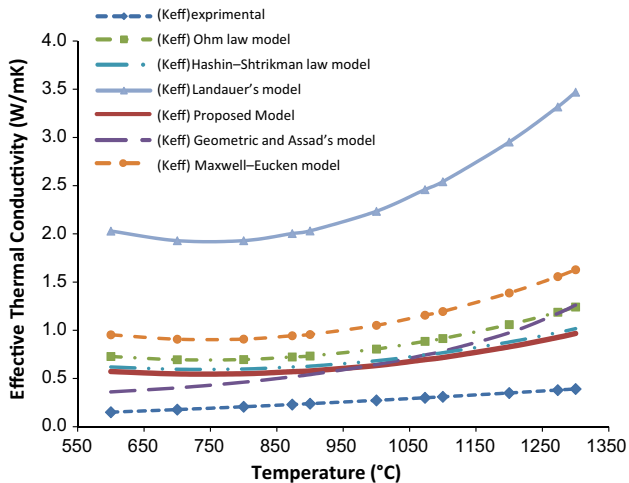


Fig. 10 Comparison of predicted effective thermal conductivity for insulator K26_AC3 by different models and the experimental measurements

theoretical models same as other samples. Figures 10 and 11 showed the good agreement between developed model's results and experimental data. SDs of different models confirm the accuracy of developed model.

4 Conclusions

The present study focuses on the heat transfer in ceramic thermal insulator porous media. A self-consistent method is developed to achieve effective thermal conductivity for the porous medium used. The porous matrix is divided into continuous and discrete phases. This method leads to an equation for effective heat transfer coefficient containing terms of matrix and air conductivity heat transfer coefficients and porosity. In this study, two dimensionless numbers, P_{lt} (ratio of heat transfer coefficient in local thermal equilibrium to the difference between heat transfer coefficients in local thermal Non-equilibrium) and R_{nu} (Reverse Nusselt Number) were introduced. These two numbers indirectly considers effect of various parameters such as size and shape of the pores, temperature gradient, thermophysical properties, components of the dispersed phase and arrangement of dispersed phase. The model thus developed was examined against experimental data and was at the same time compared to other similar models previously developed over a wide range of insulator properties. The comparisons show good agreement over the whole of the wide range examined using SD as a criterion resulting in SD of around 0.5 % compared to more than 1 % at times for other models.

Acknowledgments The authors would like to acknowledge Prof. Farhad Golestanifard (School of Metallurgy and Materials Engineering of IUST) and Mr. Mohammad Javad Avazpour (Department of Technical Inspection, Maroon Petrochemical Co., Mahshahr, Iran) for providing us technical supports. The authors are also grateful to the Research Council of Alzahra University. We also thank the Synthesis Laboratory School of Metallurgy and Materials Engineering of IUST for their support and contribution to this study.

References

- Nield DA, Bejan A (2006) Convection in porous media, 3rd edn. Springer, New York
- Hasert M, Bernsdorf J, Roller S (2011) Lattice Boltzmann simulation of non-Darcy flow in porous media. *Proc Comput Sci* 4:1048–1057
- Kou J, Wu F, Lu H, Xu Y, Song F (2009) The effective thermal conductivity of porous media based on statistical self-similarity. *Phys Lett A* 374:62–65
- Kamseu E, Nait-Ali B, Bignozzi MC, Leonelli C, Rossignol S, Smith DS (2012) Bulk composition and microstructure dependence of effective thermal conductivity of porous inorganic polymer cements. *J Eur Ceram Soc* 32:1593–1603
- Kantorovich II, Bar-Ziv E (1999) Heat transfer within highly porous chars: a review. *Int J Fuel* 78:279–299
- Grandjean S, Absi J, Smith DS (2006) Numerical calculations of the thermal conductivity of porous ceramics based on micrographs. *J Eur Ceram Soc* 26:2669–2676
- Wang J, Carson JK, North MF, Cleland DJ (2006) A new approach to modeling the effective thermal conductivity of heterogeneous materials. *Int J Heat Mass Transf* 49:3075–3083
- Park YK, Lee JK, Kim JG (2008) A new approach to predict the thermal conductivity of composites with coated spherical fillers and imperfect interface. *Int J Mater Trans* 49:733–736
- Bourret J, Tessier-Doyen N, Nait-Ali B, Pennec F, Alzina A, Peyratout CS, Smith DS (2013) Effect of the pore volume fraction on the thermal conductivity and mechanical properties of kaolin-based foams. *J Eur Ceram Soc* 33:1487–1495
- Boomsma K, Poulikakos D (2001) On the effective thermal conductivity of a three-dimensionally structured fluid-saturated metal foam. *Int Commun Heat Mass Transf* 44:827–836
- Huai X, Wang W, Li Z (2007) Analysis of the effective thermal conductivity of fractal porous media. *Appl Therm Eng* 27:2815–2821
- Bhoopal RS, Sharma PK, Singh R, Kumar S (2013) Effective thermal conductivity of polymer composites using local fractal techniques. *Int J Innov Technol Explor Eng (IJITEE)* 2:95–100
- Sanjaya CS (2011) Pore size effect on heat transfer through porous medium. Ph.D. dissertation, National University of Singapore, Singapore, Civil and Environmental Engineering
- Radhakrishnan A, Lu Z, Kandlikar SG (2010) Effective thermal conductivity of gas diffusion layers used in PEMFC: measured with guarded-hot-plate method and predicted by a fractal model. *ECS Trans* 33:1163–1176
- Tariku F, Kumaran K, Fazio P (2010) Transient model for coupled heat, air and moisture transfer through multi layered porous media. *Int J Heat Mass Transf* 53:3035–3044
- Versteeg HK, Malalasekera W (2007) An introduction to computational fluid dynamics, 2nd edn. Pearson Education Limited, Harlow
- Bejan A (1995) Convection heat transfer, 2nd edn. Wiley, New York
- Vafai K (2005) Handbook of porous media, 2nd edn. Taylor & Francis Group LLC, Boca Raton
- Yang K, Vafai K (2011) Analysis of heat flux bifurcation inside porous media incorporating inertial and dispersion effects—an exact solution. *Int J Heat Mass Transf* 54:5286–5297
- Nield DA (2012) A note on local thermal non-equilibrium in porous media near boundaries and interfaces. *Transp Porous Media* 95:581–584
- Yang K, Vafai K (2010) Analysis of temperature gradient bifurcation in porous media—an exact solution. *Int J Heat Mass Transf* 53:4316–4325
- Minkowyc WJ, Haji-Sheikh A, Vafai K (1999) On departure from local thermal equilibrium in porous media due to a rapidly changing heat source: the Sparrow number. *Int J Heat Mass Transf* 42:3373–3385
- Khezrabadi MN, Naghizadeh R, Assadollahpour P, Mirhosseini SH (2007) An investigation on the properties and microstructure of mullite-bounded cordierite ceramics. *J Ceram Process Res* 8:431–434
- Kamseu E, Nait-Ali B, Bignozzi MC, Leonelli C, Rossignol S, Smith DS (2012) Bulk composition and microstructure dependence of effective thermal conductivity of porous inorganic polymer cements. *J Eur Ceram Soc* 32:1593–1603
- Barrios M, Van Sciver SW (2013) Thermal conductivity of rigid foam insulations for aerospace vehicles. *Cryogenics* 55:12–19
- Tseng CJ, Yamaguchi M, Ohmori T (1997) Thermal conductivity of polyurethane foams from room temperature to 20 K. *Cryogenics* 37:305–312
- Stewart J (1994) The influence of morphology on polyurethane foam heat transfer. Master of Science dissertation, Massachusetts Institute of Technology, Massachusetts, Mechanical Engineering
- Goodson CC (1997) Simulation of microwave heating of mullite rods. Master of Science dissertation, Virginia Polytechnic Institute and State University, Virginia, Mechanical Engineering
- Clauser C (2011) Thermal storage and transport properties of rocks, I: Heat capacity and latent heat, encyclopedia of solid earth geophysics, 2nd edn. Springer, Dordrecht
- Takeda M, Onishi T, Nakakubo S, Fujimoto S (2009) Physical properties of iron-oxide scales on Si-containing steels at high temperature. *Mater Trans* 50:2242–2246
- Mahbulul IM, Fadhilah SA, Saidur R, Leong KY, Amalina MA (2013) Thermo physical properties and heat transfer performance of Al₂O₃/R-134a nanorefrigerants. *Int J Heat Mass Transf* 57:100–108